J. Am. Chem. Soc. **1990**, *112*, 8230-8238

Polyisocyanides: Electronic or Steric Reasons for Their Presumed Helical Structure?

Christian Kollmar and Roald Hoffmann*

Contribution from the Department of Chemistry and Materials Science Center, Cornell University, Ithaca, New York 14853-1301. *Received December 11, 1989*

Abstract: Molecular orbital calculations of the electronic structure of planar all-trans polyisocyanide point to a balance of π delocalization and N lone-pair repulsion as important structure-determining factors. The lone-pair repulsion dominates and favors a departure from planarity. Analogous considerations apply to oligo- and polyketones. Calculations on RNC helices [R = H, CH_3, $C(CH_3)_3$] show that the bulk of the R group influences the helical angle adopted. There is a fairly broad range of helical conformations available for the hypothetical R = H polymer, which sharpens to a narrow range around the 4-fold helix as the steric bulk of the substituent grows. For intermediate steric bulk, e.g., R = CH_3, we obtain an intriguing result in the theoretical conformational analysis—two helical minima with different degrees of helicity.

1. Introduction

Polymers with helical structures, both organic and inorganic, have been known for a long time.[1] Inorganic examples are elemental sulfur for which, among others, a helical allotrope exists,[2] and selenium, which forms 3-fold helical chains.[3] Helical subunits also exist in some binary compounds such as CsSb[4] and NaP,[5] where the Sb and P atoms form 4-fold helical chains. In the organic field, we find a polymer as common as polyethylene adopting a helical structure[6] besides the well-known all-trans structure. Of course, there also exist helical biopolymers, e.g., polypeptides[7] and α helices[8] in proteins and DNA.[9]

Theoretical investigations of helical polyethylene have been performed by Imamura and Fujita.[10] These authors have pioneered in adapting the extended Hückel and CNDO/2 methods to systems with helical symmetry. Very recently, Cui and Kertesz[11] examined some of the polymers mentioned above using extended Hückel and MNDO molecular orbital (MO) methods.

The helical polymers we are concerned with in the present paper are the polyisocyanides, the repeat unit of which is shown in **1**.

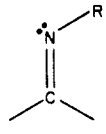

1

R is usually a rather large substituent. Millich[12] suggested a rigid rod 4-fold helical structure for these polymers (**2**). Precise structural details for these polymers are not yet available. An attractive hypothesis for a possible polymerization mechanism for polyisocyanides catalyzed by nickel(II) chloride has been given by Drenth.[13]

While the 4/1 helical nature of the polyisocyanides is widely cited, we should note that an important recent paper by Green et al.[15] has presented cogent reasons for reexamining the generality

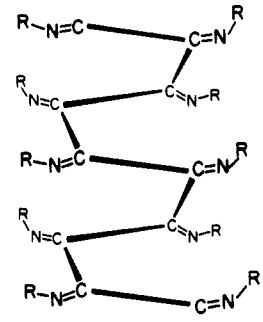

2

of this view. NMR studies, which show substantial carbon chemical shift dispersion, and circular dichroism measurements argue for some stereoirregularity and lack of stiffness in polyisocyanides, at least for some R groups.[15]

Why might these polymers be helical? According to Millich,[12] steric reasons and a more favorable alignment of electrical dipole moments should be the driving force for helix formation. We want to test this hypothesis by looking into the electronic structure of the polyisocyanides as a function of R. Actually, we have reason to suspect that the helical structure might be an intrinsic chain effect rather than a steric consequence of the substituents. It is well-known that the polyketones, whose carbonyl group is isoelectronic with the isocyanide ligand, prefer dihedral angles not far from 90° within the CCCC main chain and, thus, also adopt a helical structure,[14] though there seems to be no steric hindrance to a planar structure, e.g., of $CH_3COCOCOCH_3$.

Thus, in a first step, we examine the electronic structure of planar all-trans polyisocyanide (**3**), with the smallest model ligand

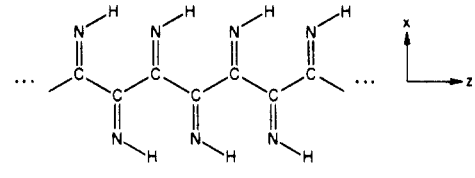

3

H. If we are able to find electronic reasons for avoiding that structure, then there is no choice other than to adopt a helical structure if a regular polymeric array is to be retained. It should be noted that we have not examined breaks in the regularity of the planar or helical polymers arising from possible syn-anti isomerism around the CN bond. We will then proceed to study such helices, and to vary the substituent R. The calculations are done within the framework of a tight-binding version[16a] of the

(1) Vogl, O.; Jaycox, G. D. *Polymer* **1987**, *28*, 2179.
(2) Donohue, J. *The Structure of the Elements*; Robert E. Krieger Publishing Co.: Malabar, FL, 1982; pp 346 ff.
(3) Cherin, P.; Unger, P. *Inorg. Chem.* **1967**, *6*, 1589.
(4) Von Schnering, H. G.; Hönle, W.; Krogull, G. *Z. Naturforsch.* **1979**, *B34*, 1678.
(5) Von Schnering, H. G.; Hönle, W. *Z. Anorg. Allg. Chem.* **1979**, *456*, 194.
(6) Kavesh, S.; Schultz, J. M. *J. Polym. Sci., Part A-2* **1970**, *8*, 243.
(7) Walton, A. G. *Polypeptides and Protein Structure*; Elsevier North Holland Inc.: New York, 1981.
(8) Pauling, L.; Corey, R. B. *Proc. Natl. Acad. Sci. U.S.A.* **1951**, *37*, 235.
(9) Walton, A. G.; Blackwell, J. *Biopolymers*; Academic Press: New York, 1973.
(10) (a) Imamura, A. *J. Chem. Phys.* **1970**, *52*, 3168. (b) Fujita, H.; Imamura, A. *J. Chem. Phys.* **1970**, *53*, 4555.
(11) Cui, C. X.; Kertesz, M. *J. Am. Chem. Soc.* **1989**, *111*, 4216.
(12) Millich, F. *Adv. Polym. Sci.* **1975**, *19*, 117.
(13) Drenth, W.; Nolte, R. J. M. *Acc. Chem. Res.* **1979**, *12*, 30.
(14) Rubin, M. B. *Chem. Rev.* **1975**, *75*, 177.
(15) Green, M. M.; Gross, R. A.; Schilling, F. C.; Zero, K.; Crosby, C., III *Macromolecules* **1988**, *21*, 1839.

0002-7863/90/1512-8230$02.50/0

extended Hückel theory[16b] (see Appendix), except for the conjugated π system of the all-trans structure, which in a first approach is treated by simple Hückel theory.

2. The Conjugated π System of All-Trans Polyisocyanide in a Hückel Model

Looking at the all-trans structure (**3**) of polyisocyanide one might wonder if the conjugated π system is a stabilizing factor for the planar arrangement, i.e., if it provides for some π bonding between the C atoms of the main chain. This question can be resolved qualitatively by a simple Hückel calculation. Considering the translational symmetry of **3**, there are two CNH units per unit cell. But since simple Hückel theory takes into account only nearest neighbor interactions, we can forget about the real geometry of the molecule and consider only its topology. This allows us to restrict our considerations to one CNH unit per unit cell, thus reducing the number of π bands in the first Brillouin zone from 4 to 2.

It is necessary to make assumptions about the Hückel α (Coulomb integral) and β (resonance integral) parameters in the case of heteroatoms. The following relations obtain for a nitrogen heteroatom:[17]

$$\alpha_N = \alpha_C + h_N\beta_0 \qquad (h_N \approx 0.5)$$
$$\beta_{CN} = f_{CN}\beta_0 \qquad (f_{CN} \approx 1) \tag{1}$$

β_0 is the resonance integral for a C–C π bond, whereas β_{CN} refers to the C–N π bond. In the second equation we have used the letter f instead of the familiar k, wishing to reserve k for the wave vector of the Bloch sums in our case. Using the Bloch sums

$$|\phi_C(k)\rangle = \frac{1}{\sqrt{N}}\sum_n e^{ikna}|\phi_{C,n}\rangle$$
$$|\phi_N(k)\rangle = \frac{1}{\sqrt{N}}\sum_n e^{ikna}|\phi_{N,n}\rangle \tag{2}$$

we obtain the following secular matrix of the Hamiltonian:

	$\lvert\phi_C(k)\rangle$	$\lvert\phi_N(k)\rangle$
$\langle\phi_C(k)\rvert$	$\alpha_C + 2\beta_0 \cos ka$	$f_{CN}\beta_0$
$\langle\phi_N(k)\rvert$	$f_{CN}\beta_0$	$\alpha_N + h_N\beta_0$

(3)

with energy eigenvalues

$$E(k) = \alpha_C + \beta_0\left\{\cos ka + \frac{h_N}{2} \pm \sqrt{\left(\cos ka - \frac{h_N}{2}\right)^2 + f_{CN}^2}\right\} \tag{4}$$

and eigenfunctions

$$|\pi(k)\rangle = \cos\frac{\omega}{2}|\phi_C(k)\rangle - \sin\frac{\omega}{2}|\phi_N(k)\rangle$$

$$\tan\omega = \frac{f_{CN}}{\cos ka - \frac{h_N}{2}} \tag{5}$$

$$|\pi^*(k)\rangle = \sin\frac{\omega}{2}|\phi_C(k)\rangle - \cos\frac{\omega}{2}|\phi_N(k)\rangle$$

The angle ω has no real physical significance. It is simply introduced to avoid otherwise messy expressions for the wave functions. The energy bands and the corresponding π wave function according to eq 4 and 5 are shown in Figure 1a and **4**, respectively. Since the C and N atoms contribute one π electron each, the π band is full and the π^* band is empty, which provides us with a strong C–N π bond.

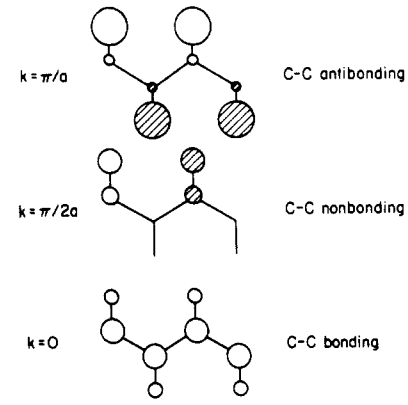

4

One important question for us is whether there is also some π bonding in the C–C main chain. Were the distribution of the orbital coefficients among the C and N atoms the same throughout the Brillouin zone, there would be no C–C π bonding in the Hückel scheme. Taking into account the overlap, as is the case in the extended Hückel method, there would even be a slightly antibonding π interaction within the C–C main chain, because a full band comprised of the same orbital (in our case a C–N π bonding orbital) yields an overall antibonding interaction, in analogy to a two-orbital four-electron interaction in the molecular case.[18] But, actually, we have a k-dependent mixture of C–N π and π^* orbitals. It is possible to show this by choosing Bloch sums for the π and π^* orbitals as a starting basis instead of atomic p orbitals as has been done in eq 2. Setting up the secular matrix then would yield a k-dependent interaction term between π and π^*, mixing the two orbitals. The mixing occurs in such a way that there is a continuous decrease of the C coefficient and a corresponding increase in the N coefficient as k increases from 0 to π/a. This can be seen from eq 5 and **4**. **4** also shows us that the C–C interaction is bonding between $k = 0$ and $k = \pi/2a$, nonbonding at the latter k point, and antibonding between $k = \pi/2a$ and $k = \pi/a$. This can be verified easily by considering the phase factor e^{ika} between neighboring unit cells occupied by neighboring C atoms. Due to the decreasing C orbital coefficient with increasing k, the bonding in the first half of the Brillouin zone is not completely compensated by the antibonding in the second half. This leaves us with a net effect of some C–C π bonding, stabilizing the planar all-trans arrangement. But, to be sure, this stabilizing effect is much smaller than, e.g., the stabilization of the planar structure of polyacetylene by its π system.

After these simple considerations we proceed to an extended Hückel calculation for planar all-trans polyisocyanide. Here, in contrast to the simple Hückel method, we cannot rely on just the topology of the molecule but have to take into account the real geometrical arrangement of the atoms. Thus, making use of the translational symmetry, we end up with two isocyanide units per unit cell, in contrast to the single unit of the previous calculation. This doubling of the unit cell will halve the Brillouin zone and lead to a "folding back" of the bands.[18] The resulting band structure, at the Hückel level, is shown in Figure 1b. Please note that there are no new interactions here—parts a and b of Figure 1 show exactly the same energy levels, but with two different choices of a unit cell. This is also indicated by denoting the wave vector as $\mathbf{k}'$ for the doubled unit cell.

3. Helical Symmetry

It turns out that the doubling of the unit cell that we have just invoked can be avoided, and an interesting generalization made, if we think a little bit more about the symmetries of these polymers. Looking at **3**, we easily recognize that this structure, in addition to the translational symmetry, also has a 2-fold screw axis as a symmetry element. A screw axis is the characteristic symmetry

(16) (a) Whangbo, M.-H.; Hoffmann, R.; Woodward, R. B. *Proc. R. Soc., London A* **1979**, *366*, 23. (b) Hoffmann, R. *J. Chem. Phys.* **1963**, *39*, 1397; Hoffmann, R.; Lipscomb, W. N. *J. Chem. Phys.* **1962**, *36*, 2179.

(17) Streitwieser, A. *Molecular Orbital Theory for Organic Chemists*; John Wiley & Son, Inc.: New York, 1962; pp 120 ff.

(18) Hoffmann, R. *Solids and Surfaces: A Chemist's View of Bonding in Extended Structures*; VCH Publishers Inc.: New York, 1989; p 8.

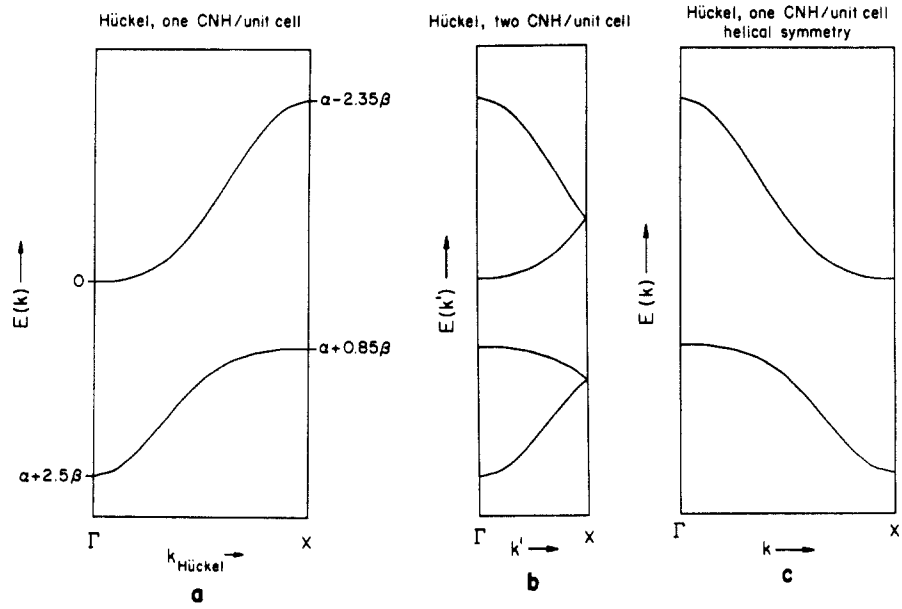

Figure 1. Hückel band structure for planar all-trans isocyanide, using the topology only (a), with the real translational symmetry of the polymer resulting in a doubling of the unit cell and a "folding back" of the bands (b), and using helical symmetry (c).

element of a helix. Thus, we consider the all-trans structure **3** as a helix with a helical angle θ of 180°. The definition of the helical angle θ is given in **5**. This approach suggests itself because below we will have to deal with nonplanar helices anyway.

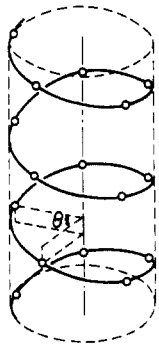

5

It has been shown that, from a group theoretical point of view, systems with helical symmetry can be treated analogously to systems with translational symmetry.[10,19] Helical symmetry is characterized by screw axis operators $\hat{S}_n(q)$ bringing the system into coincidence with itself. The operator $\hat{S}_1(q)$ represents a rotation by a fraction $0 < q < 1$ of 2π followed by a translation a. The index n refers to successively performing $\hat{S}_1(q)$ n times. The characters of the irreducible representations of the screw axis group are e^{ikna} for the operator $\hat{S}_n(q)$, using k as a label for the irreducible representation in order to show the analogy to the case of translational symmetry. Thus, the projection operators projecting the irreducible contributions out of an arbitrary wave function are obtained as follows:

$$\hat{P}_k = \sum_n e^{iknq}\hat{S}_n(q) \tag{6}$$

These look the same as in the case of translational symmetry except for the translational operators $\hat{t}_n$ now being replaced by the screw axis operators. Applying (6) to an orbital χ in any unit cell yields the Bloch sum in the usual way:

$$\psi_k = \sum_n e^{iknq}\chi_n \tag{7}$$

χ_n is the orbital χ in unit cell n. This type of Bloch function is called a pseudo Bloch function in order to distinguish it from the translational Bloch functions. Note that helical systems with rational q have translational symmetry in addition to helical symmetry, but with a usually much larger number of basic units in one unit cell. Thus, it is always preferable to use the helical symmetry.

In contrast to pure translational operators, use of the screw axis operators changes the orientation of orbitals in different unit cells. This is due to the inclusion of a rotational part in the screw axis operator. Choosing the z axis as screw axis, we obtain the following relations for orbitals differing by n unit cells:

$$\begin{aligned} p_x(n) &= p_x(0)\cos n\theta = p_y(0)\sin n\theta \\ p_y(n) &= -p_x(0)\sin n\theta = p_y(0)\cos n\theta \\ p_z(n) &= p_z(0) \end{aligned} \tag{8}$$

The s orbital, of course, is not affected. We have omitted relations for d orbitals, because we do not have them in our system. Please note that eq 8 refers only to the rotational part of the screw axis operator, thus giving us the relative orientation of orbitals in different unit cells. It does not contain the translation of the orbitals.

Now let us return to the all-trans structure and see how the Hückel approximation levels emerge when proper account is taken of the helical symmetry. The bands of Figure 1b are "unfolded" in Figure 1c. According to the coordinate system in **3**, the conjugated π system consists of p_y orbitals. The helical angle θ being 180°, it can be seen from eq 8 that the p_y orbital changes its sign when we proceed from one unit cell to its nearest neighbor. This is due to the 180° rotation involved in the screw axis operation, thus changing the sign of the p_y orbitals. The consequences for the shape of the bands are significant. Due to the opposite sign, the overlap integral of neighboring p_y orbitals is negative. Hence, at $k = 0$, we obtain a linear combination of p_y orbitals with maximum antibonding, whereas the linear combination at $k = \pi/a$ has maximum bonding. This is why the π and π^* bands in Figure 1c are running "down", whereas those in Figure 1a are running "up". It is important to realize that these figures represent the very same orbitals, just plotted in a different way. From hereon in the paper we will use the helical symmetry representation.

4. All-Trans Polyisocyanide in an Extended Hückel Model

Before entering the calculation some assumptions about the geometry of the molecule have to be made. We have chosen C—C bond lengths of 1.5 Å, C=N bond lengths of 1.3 Å, and N—H bond lengths of 1.0 Å. These bond lengths are kept constant

(19) (a) Ukrainskii, I. I. *Theor. Chim. Acta* **1975**, *38*, 139. (b) Blumen, A.; Merkel, C. *Phys. Status Solidi B* **1977**, *83*, 425.

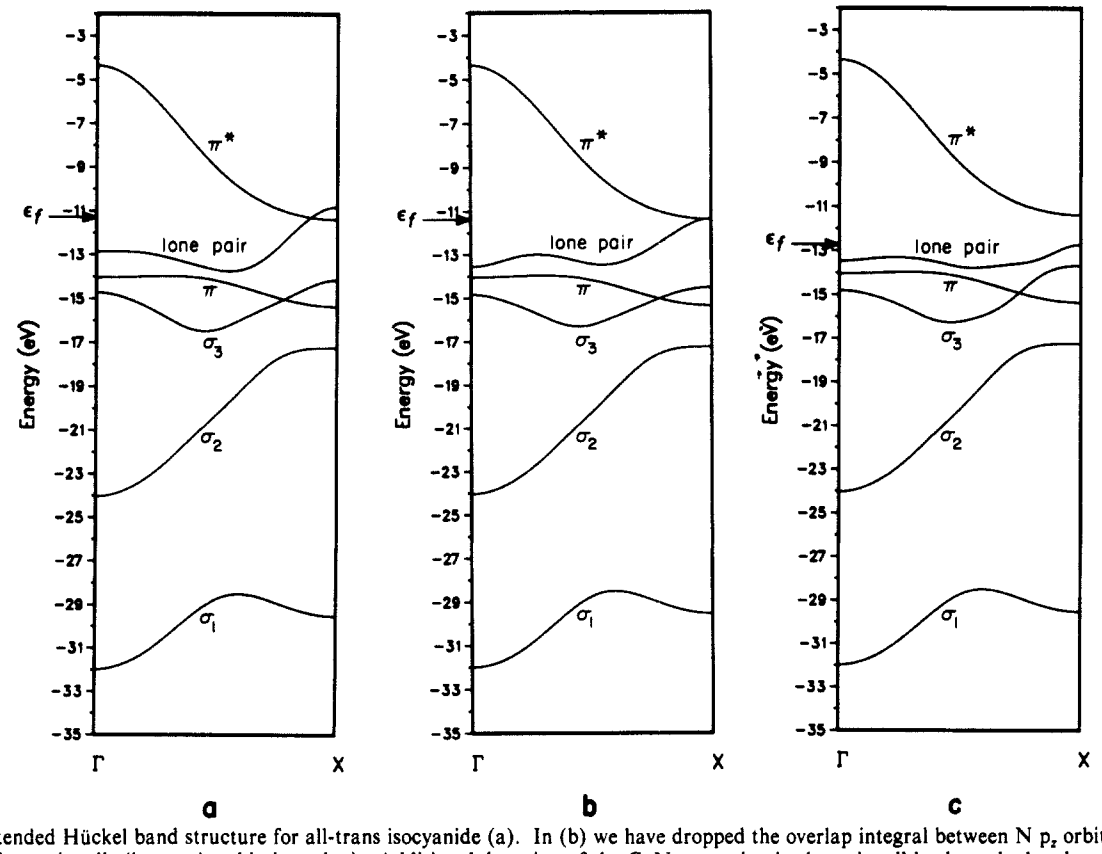

Figure 2. Extended Hückel band structure for all-trans isocyanide (a). In (b) we have dropped the overlap integral between N p_z orbitals in second nearest neighbor unit cells (lone-pair orbital overlap). Additional dropping of the C–N p_z overlap in the unit cell leads to the band structure of (c).

throughout all our calculations. Moreover, the C–C–C angle within the main chain and the C–N–H bending angle are both chosen as 120°. The resulting extended Hückel band structure is shown in Figure 2a.

The bands below the π band are σ levels. Most importantly, there is a nitrogen lone-pair band (more on this below), which is above the π band. The lone-pair band even intersects the π^* band, implying metallic behavior for this geometry of the polymer within our model. In general, the π and π^* bands are "running down", as predicted from our simple Hückel considerations. Nevertheless, there is an interesting detail concerning the π band. Looking carefully at this band in Figure 2a, we recognize that at the beginning of the Brillouin zone it runs slightly up. This is due to second nearest neighbor interactions, which are not included in the simple Hückel method. The term second nearest neighbor here refers to the numbering of unit cells when using helical symmetry, i.e., second nearest neighbors in **3** are neighboring CNH units on the same side of the polymer chain. Note that we do not have to care about the rotational part of the screw axis operator in the case of second nearest neighbors, because the corresponding rotational angle amounts to 360° (see eq 8 with $n = 2, \theta = 180°$). The phase shift between the orbital coefficients of second nearest neighbors in the Bloch sums is e^{i2ka}. Thus, this interaction is bonding at $k = 0$ (Γ) and $k = \pi/a$ (X). But there is an antibonding area in the middle of the Brillouin zone around $k = \pi/2a$, because the phase factor there is −1. These phase shifts can also be seen in **4**. Hence, the second nearest neighbor interaction causes a downshift of the energy levels near the edges Γ and X of the Brillouin zone and an upshift in the center of the Brillouin zone, thus explaining the peculiar shape of the π band in Figure 2a. This was probed by dropping the overlap integrals between p_π orbitals in neighboring unit cells, thus leaving us only with second and higher nearest neighbor interactions. In that case, there would be no dispersion for the simple Hückel scheme. The resulting extended Hückel band structure (not shown here) confirms our hypothesis by showing energy minima for the π band at the edges Γ and X of the Brillouin zone and a maximum at the center. It should also be noted that, in contrast to the first neighbor interaction, which takes place within the C–C main chain, not only the C atoms but also the N atoms contribute significantly to the second nearest neighbor interaction, as can be seen from **3**.

In still another numerical experiment, dropping the overlap integrals between all p_π orbitals except for those within the same unit cell allows us to assess the energy stabilization of the planar all-trans structure due to the delocalization within the conjugated π system. Without the inter-unit-cell p_π overlap the system is destabilized by 206 meV per unit cell. Please note that the energy stabilization of the conjugated system is not only due to C–C bonding in the π band but can also be partly ascribed to the ability of the system to dump some of its lone-pair electrons into the C–C bonding part of the π^* band (note the overlap between the lone pair and π^* bands in Figure 2a, which also renders this system metallic). We can extract the pure effect of the π band by emptying the lone-pair band, thus avoiding the partial occupation of the π^* band. We find that 125 meV of the total energy stabilization of 206 meV can be attributed to the π band. We want to emphasize that these energy values are by no means accurate numbers. They only should provide us with some hints about the order of magnitude of the effects evolving in the analysis of the band structure.

5. The Role of the Nitrogen Lone Pair

Let us now take a look at the N lone-pair band falling between the π and π^* bands in Figure 2a. The orbital composition of this band at Γ and X is shown in **6**. We recognize that it is a very

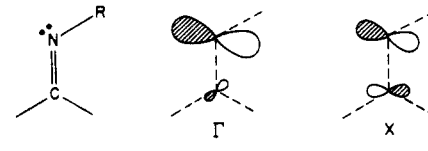

6

good lone pair at Γ, whereas there is considerable contribution of the C p_z orbital at X. The s contribution to the lone-pair orbital can be neglected; it is an almost pure p orbital. Thus, given the second nearest neighbor N–N distance of only ~2.6 Å in **3**, we

can expect considerable through-space interaction of the corresponding lone-pair orbitals. We have already seen that second nearest neighbor interaction shows up in the bands of the conjugated π system. Moreover, the orientation of the p orbitals in **6** makes them suitable for favorable overlap. Thus, it seems justified to ask about the possibility of lone-pair repulsion in the all-trans structure of polyisocyanide.

To analyze the N lone-pair repulsion in this system we first perform an analytical calculation for an "idealized" lone-pair band with the lone pairs consisting of pure N p_z orbitals, as shown in **7**. What does the band structure of such an orbital configuration

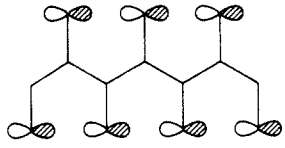

7

look like? We again use the helical symmetry with one isocyanide unit per unit cell. The Bloch sums for the lone-pair orbitals are written in the usual way:

$$|p_z(k)\rangle = \sum_n e^{ikna}|p_{z,n}\rangle \tag{9}$$

Note that the p_z orbitals are not affected by the rotational part of the screw axis operator as can be seen from eq 8. The energy in the tight binding approximation is obtained by forming

$$E(k) = \frac{\langle p_z(k)|\hat{H}|p_z(k)\rangle}{\langle p_z(k)|p_z(k)\rangle} \tag{10}$$

It is important to include the overlap between neighboring p_z orbitals explicitly in the normalization factor in the denominator. That is why we have not put the usual normalization factor $1/N^{1/2}$ in front of the Bloch sum on the right side of eq 9 but have included the normalization in the energy term 10. Inserting (9) into (10) and taking into account interaction and overlap up to the second nearest neighbors we obtain

$$E(k) = \frac{h_{11} + 2h_{12}\cos ka + 2h_{13}\cos 2ka}{1 + 2S_{12}\cos ka + 2S_{13}\cos 2ka} \tag{11}$$

with

$$h_{11} = \langle p_{z,n}|\hat{H}|p_{z,n}\rangle$$

$$h_{12} = \langle p_{z,n}|\hat{H}|p_{z,n+1}\rangle \qquad S_{12} = \langle p_{z,n}|p_{z,n+1}\rangle \tag{12}$$

$$h_{13} = p_{z,n}|\hat{H}|p_{z,n+2}\rangle \qquad S_{13} = \langle p_{z,n}|p_{z,n+2}\rangle$$

In order to refer all the energy levels to the ionization potential α, eq 11 can be rewritten:

$$E(k) = \alpha + \frac{2\beta_{12}\cos ka + 2\beta_{13}\cos 2ka}{1 + 2S_{12}\cos ka + 2S_{13}\cos ka} \tag{13}$$

with

$$\alpha = h_{11} \qquad \beta_{12} = h_{12} - h_{11}S_{12} \qquad \beta_{13} = h_{13} - h_{11}S_{13} \tag{14}$$

Now it can be seen from **7** that the distance between nitrogen atoms in neighboring unit cells is much larger than the second nearest neighbor distance. Thus, we neglect S_{12} and β_{12} in (13), ending up with

$$E(k) = \alpha + \frac{2\beta_{13}\cos 2ka}{1 + 2S_{13}\cos 2ka} \tag{15}$$

A schematic band structure plot according to eq 15 is shown in Figure 3. Now the effect of including the overlap integral in the denominator can be discerned easily: The upshift in energy of the antibonding levels with respect to α is stronger than the downshift of the bonding levels, leading to an overall destabilization. This is the N lone-pair repulsion we have been looking for. It is completely analogous to a two-orbital four-electron interaction in the molecular case.[18] The amount of energy destabilization per N atom can be calculated by integration of the band energy over the Brillouin zone

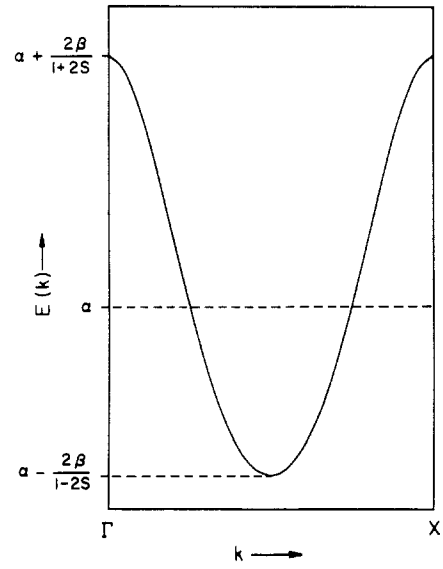

Figure 3. Schematic band structure for an idealized lone-pair orbital of all-trans polyisocyanide.

$$E_{\text{total}} = \frac{2}{N}\int_{-\pi/a}^{\pi/a} E(k)\rho(k)\,dk \tag{16}$$

where N is the number of nitrogen atoms and the factor 2 accounts for the double occupation of each energy level. ρ is the density of states:

$$\rho(k) = Na/2\pi \tag{17}$$

Inserting eqs 15 and 17 into 16 and expanding the denominator of (15) in a Taylor series, which is terminated after the second term, the integral in (16) can be calculated analytically. We end up with

$$E_{\text{total}} = 2\alpha - 4\beta_{13}S_{13} \tag{18}$$

The first term refers to the energy of a doubly occupied nitrogen p orbital. The destabilization is given by the second term. We can see from **7** that the overlap integral S_{13} is negative. Consequently, β_{13} is positive, leading to an overall positive sign characteristic of a destabilization. Assuming $\beta_{13} \sim S_{13}$, the destabilization is proportional to the square of the overlap integral, a result again analogous to the two-orbital four-electron molecular case.[20]

Thus far our considerations have been very schematic. Does the effect just described show up in the real band structure? Looking at Figure 2a we recognize that the lone-pair band is indeed similar in shape to our schematic band structure of Figure 3, though there is some deviation, especially near X. The reason for the asymmetric shape of the real band structure with the upshift of the energy levels near X can be seen from **6**: whereas at Γ our idealized lone pair is a good approximation, this is no longer the case near X. A C p_z orbital mixes in in an antibonding manner, thus causing the upshift in energy. Nevertheless, the shape of the lone-pair band suggests that the second nearest neighbor repulsion is important. We confirmed this hypothesis by a numerical experiment, dropping the overlap integral between p_z orbitals of nitrogen second nearest neighbors. The resulting band structure is shown in Figure 2b. It can be easily imagined that superimposing a curve of the shape of Figure 3 upon the lone-pair band of Figure 2b results in the lone-pair band of Figure 2a. This indicates the significance of the second nearest neighbor effect.

The effect just described results from a direct through-space interaction of lone-pair orbitals in second nearest neighbor unit

(20) Albright, T. A.; Burdett, J. K.; Whangbo, M.-H. *Orbital Interactions in Chemistry*; John Wiley & Sons: New York, 1985; pp 12 ff.

cells. Another important interaction frequently occurring between lone-pair orbitals is through-bond interaction,[21] in our case by means of the σ backbone of the polymer. This can be probed by dropping the overlap intergral between the p_z orbitals of C and N in the same unit cell, in addition to the forementioned second nearest neighbor N–N p_z overlap. The resulting band structure is shown in Figure 2c. Now an avoided crossing between the band σ_3 and the lone-pair band occurs near X. Thus at X, the band labeled σ_3 is actually the lone-pair and vice versa. σ_3 has dominant C p_z character at X and provides for C–C σ bonding in the main chain (**8**). The lone-pair band, on the other hand, is predomi-

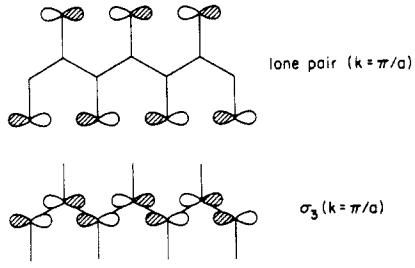

8

nantly localized on the nitrogen as shown in **8**. Except in the region of the avoided crossing, it is a very flat band now, because we have eliminated the relevant through-space and through-bond interactions by dropping the overlap integrals. "Switching on" the interaction between the carbon and nitrogen p_z orbitals results in the band structure of Figure 2b. Since the bands are close in energy they mix strongly near X, thus repelling each other (compare parts b and c of Figure 2). The high-energy antibonding linear combination of the orbitals shown in **8** results in the orbital shown in **6** on the right. The band σ_3 is shifted down in energy near X and acquires considerable N p_z character due to the bonding linear combination of the orbitals in **8**.

Why does the lone-pair orbital remain pure at Γ? This is due to the fact that the relevant σ orbital that could mix with the lone-pair combination is now a C–C antibonding orbital (see **9**),

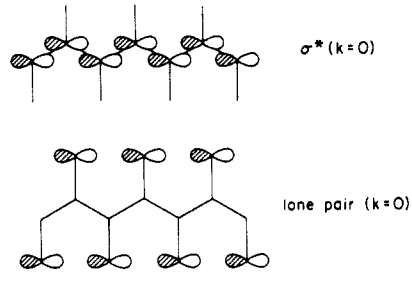

9

which is too high in energy to achieve considerable mixing with the lone pair. The phenomenon follows a pattern typical for through-bond coupling, a symmetry-differentiated capability for interaction.

We turn to some quantitative energy assessments. Dropping the N–N p_z overlap integral leads to an energy gain of 247 meV per unit cell. Please note that the effect is very sensitive to the overlap of the lone-pair and π^* bands, which cross each other near X. The general experience with extended Hückel calculations on organic molecules is that the σ levels come out a little to high in energy relative to the π levels. Thus, we cannot take the band overlap for granted. If the lone-pair band were fully occupied, the lone-pair repulsion would be increased by 81 meV. In order not to count the effect of band overlap twice, we thus have to compare the repulsion energy of 247 meV with the energy gain by the conjugated π system of 125 meV (without the effect of electron dumping into the π^* band; see previous section). This leaves us with a net destabilization of ~120 meV per unit cell (~200 meV without band overlap). This energy could be released if the system were to distort in a way that allows it to get rid of the close N–N second nearest neighbor contact. Conjugation in the π system would be partially or wholly lost in such a distortion. These quantitative considerations have to be taken with great caution due to the crudeness of our calculational method. Qualitatively, however, we believe that both the lone-pair repulsion and the conjugated π system are crucial features in deciding whether there are electronic reasons for avoiding the planar all-trans structure.

There is another question that needs to be addressed. Looking at the all-trans structure **3**, one might wonder if there would be a stabilizing contribution from H bonding to the nitrogen lone pair of the second nearest neighbor unit cell. It is well-known that, e.g., in polypeptide α-helices,[8] the H bridges to carbonyl groups are structure-determining factors, responsible for the helical shapes of these molecules. We have examined this question by dropping the overlap integral between the H s orbital and all the orbitals of the N atom in the second nearest neighbor unit cell. The result is surprising. Instead of a rise in energy due to the loss of the H bridge we obtain a lower energy. Though we really lose the H bonding to the second nearest neighbor N atom (indicated by a small overlap population of ~0.04), the N–H bond within the unit cell is strengthened by about the same amount. We do not know if this effect is of real physical significance or just an artifact of the extended Hückel method. Resolution of this question must be left for more elaborate computational schemes. Ab initio calculations are certainly feasible for a system with such a small unit cell. It should be noted that hydrogen bonding would be important only for an H substituent on the nitrogen. This is unrealistic; the known polymers carry other R groups.

6. Helical Structure of Polyisocyanide

So far our considerations have been concerned with the planar all-trans structure and the counterbalance of two competing effects, one stabilizing this structure, the other destabilizing it. Now we want to distort this structure helically and examine how this distortion affects the band structure. As already mentioned, the planar all-trans structure can be considered a helix with a helical angle of 180°. What happens when we decrease the helical angle from 180° to 90°, the experimentally observed value for the polyisocyanides?

Again, we have to make some geometrical assumptions, because little is known about the structural details from the experiments. The bond lengths are kept the same as for the all-trans structure. We also retain the bending angle of 120° for the C–N–H group and the C–C–C bond angle of 120° within the main chain. The assumption of an isocyanide bending angle of 120° is somewhat arbitrary, but the extended Hückel method is not reliable with respect to a geometry optimization of that angle. More important is the C–C–C bond angle in the main chain, because it is one essential parameter in determining the shape of the helix. We have performed an energy optimization with respect to that angle and it turns out that the angle of minimal energy is in fact 120° for the present 4-fold helix, the same value as for the all-trans structure. Even if one does not trust these calculations there is another strong point to be made. One of the few structural data available from the work of Millich[12] is the pitch of the helix, which is 4.2 Å per one complete screw turn. Assuming a helical angle of 90°, a C–C–C bond angle of 120° and a C–C bond length of 1.5 Å, geometrical considerations yield the same value of 4.2 Å, i.e., perfect agreement.

We also have to take care that the bond arrangement shown in **1** is kept planar, i.e., the rotational angle of the isocyanide group around the C=N bond with respect to the plane formed by the C atom and its nearest neighbor C atoms should be zero. Given these assumptions, the structure is completely determined. The variable considered in the following will be the helical angle θ. Decreasing this angle from 180° to 90° will increase the radius

(21) (a) Hoffmann, R.; Imamura, A.; Hehre, W. J. *J. Am. Chem. Soc.* **1968**, *90*, 1499. (b) Hoffmann, R. *Acc. Chem. Res.* **1971**, *4*, 1. (c) Gleiter, R. *Angew. Chem., Int. Ed. Engl.* **1974**, *13*, 696. (d) Paddon-Row, M. N. *Acc. Chem. Res.* **1982**, *15*, 245.

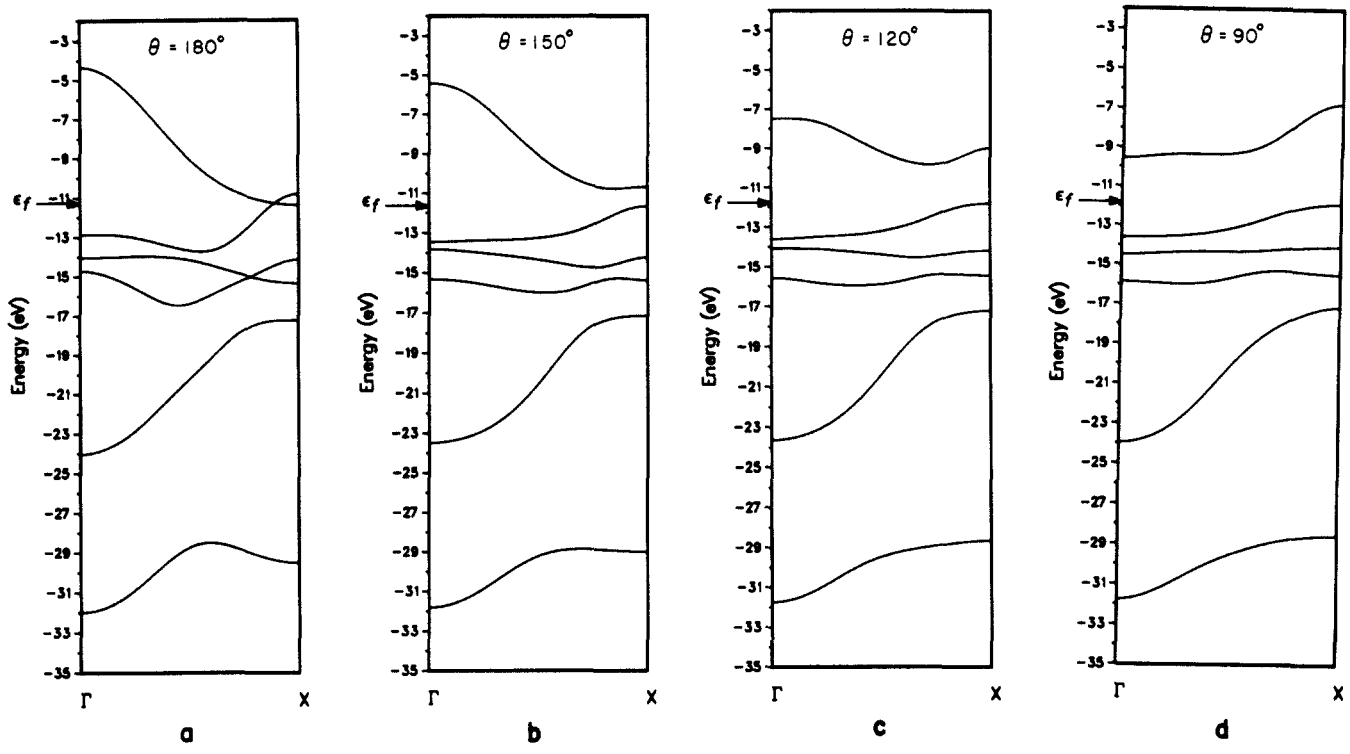

Figure 4. Band structure of polyisocyanide for various helical angles.

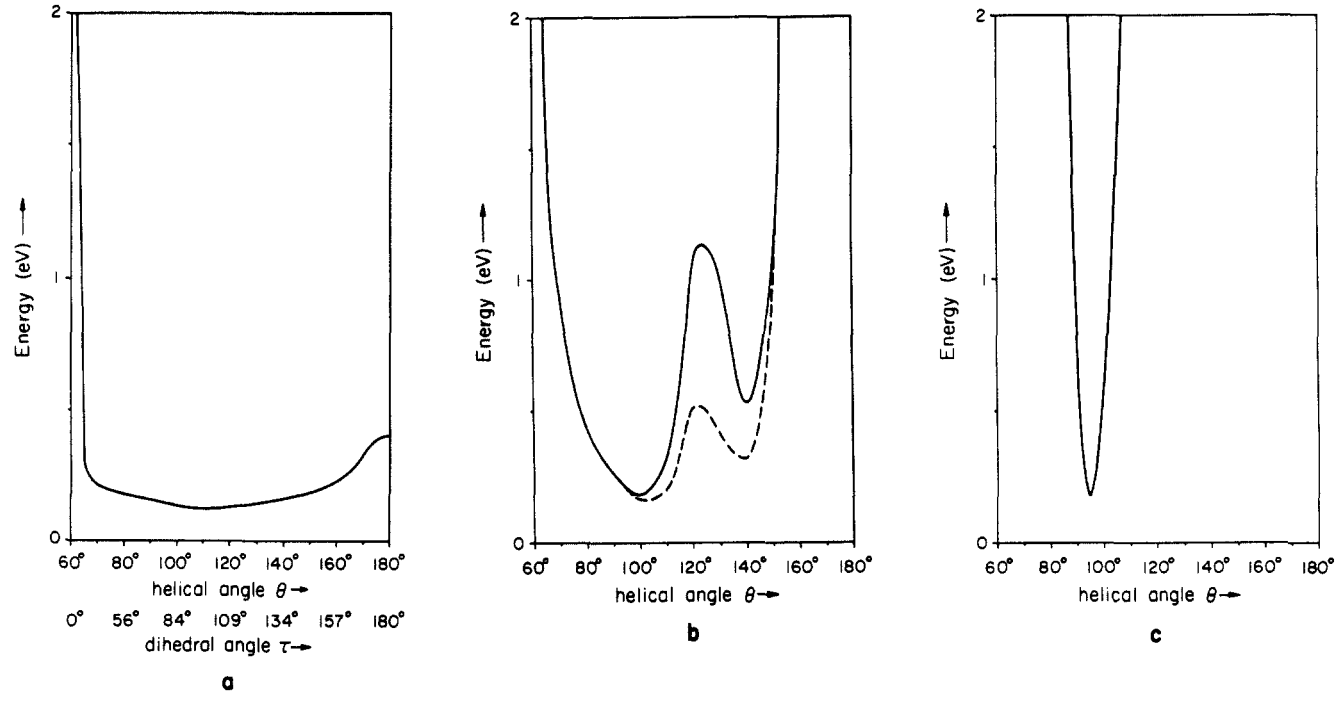

Figure 5. Total energy per unit cell as a function of the helical angle θ with H as a substituent R (a), R = CH_3 (b), and R = $C(CH_3)_3$ (c). The result for dropping the overlap integrals between N and one of the H atoms of the methyl group in (b) is given by the broken line. In (a) we have also given the corresponding dihedral angle in the main chain. The energies do not refer to the real molecular energies but have been rescaled to simple numbers because we are interested only in energy differences.

of the helix and decrease the dihedral angle from 180° to ~70°. The pitch of the helix increases, reaching a maximum at θ = 90°. On decreasing the helical angle beyond 90° the pitch is diminished, eventually reaching zero for θ = 60°. Elaborate schemes for the calculation of helix geometries can be found in the literature.[22]

We show a series of band structure plots of the polyisocyanides for different helical angles in Figure 4. It can be seen that the bands are smoothed out when the all-trans structure is abandoned. It is interesting to note that the orbital composition within the CNH unit cell for the different bands is nearly independent of the helical angle.

The energy difference between the planar all-trans structure and the helical structure with θ = 90° is 257 meV per unit cell in favor of the latter. This is higher than the net effect of the counterbalance of the two effects mentioned in the previous sections. So there might be additional effects that are not so easily traced.

We next attempted a geometry optimization with respect to the helical angle. The result is shown in Figure 5a. We recognize

(22) (a) Shimanouchi, T.; Mizushima, S.-I. *J. Chem. Phys.* **1955**, *23*, 707. (b) Yokouchi, M.; Tadokoro, H.; Chatani, Y. *Macromolecules* **1974**, *7*, 769. (c) Sugeta, H.; Miyazawa, T. *Biopolymers* **1967**, *5*, 673. (d) Miyazawa, T. *J. Polym. Sci.* **1961**, *55*, 215.

a very shallow minimum over a wide angular range from ~70° to ~150°. The rise in energy near 180° is due to second nearest neighbor nitrogens approaching each other. The steep rise for angles <70° on the other hand is caused by a decreasing distance between the threads of the helix, leading to substantial overlap between orbitals in neighboring threads. Note that for $\theta = 60°$ there would be no pitch to the helix any more, if we keep the C–C–C bond angle at 120°. All the C atoms of the helix would then collapse into the six points of a planar hexagon.

As already mentioned, the orbital composition within one CNH unit does not change very much with the helical angle, i.e., the orbitals are either perpendicular to the CNH plane (π orbitals) or oriented within this plane. Thus, it is not surprising that a dihedral angle significantly different from 0° or 180° in the C–C main chain drastically decreases the overlap of p orbitals in neighboring unit cells. This explains why the bands of the helical structure are smoothed out in comparison with the planar all-trans structure.

A nice indication of the influence of the dihedral angle in the main chain is given by the π^* band. This band is distinguished from the other bands shown in our plots by not varying very much in its orbital composition throughout the Brillouin zone and being mainly localized on the main-chain carbon atom (the π band, on the other hand, has its dominant contribution on the nitrogen). So this band is characterized by a p orbital on carbon oriented perpendicular to the plane of the atomic arrangement shown in **1**. The overlap of this orbital with its counterpart on the nearest neighbor C atom thus depends strongly on the dihedral angle. The sign and the magnitude of this overlap integral determine the direction and the band width of the π^* band, respectively. Within the range $180° > \tau > 90°$ of the dihedral angle (corresponding to the range $180° > \theta > 104.48°$ of the helical angle) the overlap integral is negative, with its maximum amount at $\tau = 180°$. This amount then decreases continuously to zero at $\tau = 90°$. Passing $\tau = 90°$ ($\theta = 104.48°$) the overlap integral changes its sign from minus to plus. Hence, the π^* band should be "running down" for $180° > \theta > 104.48°$, remain basically flat at $\theta = 104.48°$ (except for second nearest neighbor interactions, which cannot be neglected here), and "run up" for $\theta < 104.48°$. This expectation is nicely verified by Figure 4, where the direction of the π^* band is inverted between $\theta = 120°$ and $\theta = 90°$. Please note that the second nearest neighbor interaction superimposes energy shifts analogous to the shape of the curve in Figure 3 on the band structure but the general trend is reflected quite well in Figure 4.

To probe the steric effect we replace the hydrogen substituent by a CH_3 group and repeat the calculation of the total energy as a function of the helical angle. The result is shown in Figure 5b. In general, the shape of the curve is the same as in Figure 5a, but the slopes near 60° and 180° are enhanced by 1 order of magnitude. Moreover, there is a bump in the curve at ~120°. At this angle we have a 3-fold helix. Hence, an isocyanide unit and its third neighbor in consecutive order are aligned in the direction of the helical axis, just one thread apart from each other. It is therefore tempting to attribute the bump to steric effects based on this alignment. Indeed, on looking at the distance matrix, we find that one of the hydrogens of the methyl group gets as close as 1.83 and 1.77 Å to the nitrogen of the third nearest neighbor unit cell for helical angles of 120° and 130°, respectively. One would not immediately expect this close contact to be responsible for steric hindrance, for the arrangement of the atoms seems to be suitable for a hydrogen bond to the nitrogen lone pair. This can be probed by yet another numerical experiment, dropping the overlap integrals between the H atom and all orbitals of the nitrogen in the third nearest neighbor unit cell. The result is given in Figure 5b by the broken line. We encounter the same phenomenon as in the case of planar all-trans polyisocyanide: instead of an increase in energy due to the loss of the hydrogen bond we find an energy stabilization of the system in the region where we have the close N–H contact between third nearest neighbor unit cells. We thus conclude that the extended Hückel method gives a steric repulsion between N and H instead of the expected hydrogen bond. This phenomenon should be examined by more sophisticated computational methods; it is important to resolve this fundamental question because hydrogen bonds determine the shape of α helices, though in that case O atoms are involved instead of N.

The most interesting feature of the potential energy curve in Figure 5b is the existence of two minima. The deeper one is for the 4-fold helix, helical angle near 95°; the higher energy minimum near a helical angle of 140°. As far as we can tell, the coexistence of two helical conformations of the same chirality but different helical twist in one and the same polymer is not known. Temperature-dependent optical rotation is observed in polyisocyanates,[23] where it is thought to be the consequence of equilibriating enantiomeric polymer segments. It would be interesting to find a polymer with coexisting helical conformations.

We have also performed a calculation for a polyisocyanide with *tert*-butyl as a substituent, a polymer that really exists.[13] We have chosen an all-staggered arrangement for the *tert*-butyl group although some steric readjustment might take place due to the very intricately packed structure of the helix with such a bulky ligand. The result of the calculation is shown in Figure 5c. Now we have a very sharp minimum in the energy curve at an angle very close to that of the 4-fold helix ($\theta = 90°$). In order to understand why only a helix with a helical angle close to 90° is capable of relieving the multitude of possible steric interactions in the most favorable way it is necessary to look at a model of the helix. There are close N–H contacts now even in the 4-fold helix. This again raises the question of the reality of attractive or repulsive N–H interactions; these are essential for the geometrical compromises that must be made by these sterically encumbered polymers. We also did not consider a possible rotation of the substituent around the N–R bond. A proper optimization of this rotation angle as well as of the geometry within the substituent itself is likely to widen somewhat the very narrow valley in Figure 5c.

We conclude that the steric effect for substituents considerably larger than hydrogen is much stronger than the electronic effect we have been dealing with before. In the case of *tert*-butyl isocyanide it is evident from a model of the molecule that steric reasons permit only the 4-fold helical arrangement. It would seem from the sharpness of our minima that the helix should be quite stiff, though, as mentioned above, we really have not given these molecules the full range of conformational freedom.

7. Discussion and Conclusions

In the previous section we tried to outline the reasons for the adoption of a helical structure of the polyisocyanides. We began by showing that there are electronic reasons for avoiding the alternative planar all-trans structure. This led naturally to the helical structure as the only remaining possibility for a regular polymeric array.

We believe we have presented strong evidence that there is an electronic reason, a N–N repulsive interaction between nitrogens in second nearest neighbor unit cells (in helical symmetry, neighboring nitrogens on the same side of the polymer chain). These nitrogens come close to each other in the planar all-trans structure, making it energetically unfavorable. The N–N repulsion overrides the stabilizing effect of the conjugated π system. We have focused on the lone-pair band, but this repulsion is present to a smaller extent in the lowest band (s band) and in the π band as well. The effects are small in magnitude (of the order of 100 meV per unit cell) and the changes in the band structure are too complex to be reduced to these effects, putting aside the inherent crudeness of our method. But we have clearly shown that the repulsive interaction shows up in the qualitative shape of the bands and, thus, is an important part of the story.

The π system is a stabilizing factor for the planar structure in our case, though not a strong one. This is in contrast to some

(23) Lifson, S.; Andreola, C.; Peterson, N. C.; Green, M. M. *J. Am. Chem. Soc.* **1989**, *111*, 8850.

(24) See, in this context, the arguments for stereoirregularity and lack of stiffness of at least some polyisocyanides, in ref 15.

of the polymers examined by Cui and Kertesz,[11] where it is the π system that destabilizes the planar structure and leads to helix formation. This is obvious for the helices of elemental S and Se where the full π band of the planar all-trans structure is clearly repulsive, in analogy to the already mentioned two-orbital four-electron interaction.

The situation is more complicated for polyethylene. The carbons also have p orbitals perpendicular to the plane of the all-trans carbon backbone, thus forming a kind of conjugated π system. But now these orbitals mix strongly with a linear combination of H s orbitals, which is antisymmetric with respect to the backbone plane. Considering the topology of the orbitals, the situation is similar to the π system of polyisocyanide with the p_y orbital of the nitrogen in the latter case being analogous to the antisymmetric linear combination of the H s orbitals in polyethylene. Concerning the distribution of orbital coefficients between the carbon p_π orbital and the hydrogens, we then expect qualitatively the same behavior as in the case of polyisocyanide (see **4**): strong C, little H contribution for the p_π C orbitals being in-phase, and little C, strong H contributions for these orbitals being out-of-phase. Thus, the C–C bonding interaction in the bonding half of the Brillouin zone overrides the antibonding interaction in the other half, making this band a stabilizing factor for the planar arrangement. The important point is that there is not only no repulsive interaction between the C p_π orbitals in the main chain but even some weak "π" bonding between these orbitals. A repulsion would only occur if there were no shift in the orbital coefficients from carbon to hydrogen with increasing phase shift between neighboring p_π orbitals in the carbon chain. Thus, it is not at all surprising that the all-trans structure of polyethylene is the most stable one. Nevertheless, both extended Hückel[10] and MNDO[11] calculations give a second energy minimum with respect to the helical angle, at $\theta \approx 105°$ and $\theta \approx 95°$, respectively. Thus, it might be interesting to look for some qualitative reason for helix formation in polyethylene.

In the case of polyacetylene, on the other hand, it is obvious that the conjugated π system is a strong stabilizing factor for the planar arrangement of the polymer. Forgetting about the Peierls distortion and assuming equal C–C bond lengths, we have again helical symmetry. This allows us to restrict our considerations to one C–H unit per unit cell, leaving us with one half-filled π band, which provides for strong C–C π bonds. A hypothetical polyacetylene with one minus charge per CH unit, however, which would have a full repulsive π band, is expected to adopt a helical structure, in accordance with the arguments given in ref 11. Such a polymer would be isoelectronic to sulfur.

We have already stressed the similarity of the polyisocyanides to the polyketones. The spectroscopic data on the latter molecules, which exist only up to the tetramer, indicate a red shift of the $n-\pi^*$ transition with the dihedral angle increasing from 90° to 180°.[14] This is completely consistent with our results. Looking at Figure 4 we recognize that the energy gap between the lone-pair band and the π^* band decreases if the helical angle and, thus, the dihedral angle increases. At $\theta = 180°$ the two bands even overlap. This is certainly not the case for short-chain oligomers, but, nevertheless, our result is in qualitative agreement with the experimental observations for the electronically similar polyketones. The helical structure of the polyketones has been confirmed by MINDO/2 calculations.[25]

Even if long-chain polyketones do not exist, there are other important polymers containing carbonyl groups, i.e., the polypeptides.[7] They also adopt helical structures and CNDO/2 geometry optimizations have been performed.[26] No qualitative analysis of the observed geometries has been given as yet, but it is clear that hydrogen bonding, intra- (α helix) and interchain (β-pleated sheet), is essential in determining polypeptide geometries.

Summarizing, we conclude that a kind of steric hindrance of nitrogens in second nearest neighbor unit cells prevents the polyisocyanides from adopting the planar all-trans structure. This steric hindrance would probably not have been expected. It is obvious that the bulky side groups also provide for a steric effect, as argued by Millich.[12] This steric effect is much larger in magnitude than the intrinsic chain effect discussed in this paper. Steric interactions between helical loops, i.e., involving polymer units that are not nearest neighbor, become important. This is clearly seen in the computed potential energy curve as a function of helical angle for poly(methyl isocyanide) and poly(*tert*-butyl isocyanide). The principal minimum, especially for the latter polymer, is close to that of a 4-fold helix. But the helical arrangement of the isoelectronic polyketones, where no side groups are present, supports our argument that electronic reasons are important as well.

Acknowledgment. This work was made possible by a DFG grant for C.K. and was supported by NSF Research Grant CHE-8912070. We thank Jane Jorgensen and Elisabeth Fields for their expert drawings and M. M. Green for his critical comments on the structure of the polyisocyanides.

Appendix

The tight-binding extended Hückel method was used for our calculations. The k point set for the calculation of the average properties consisted of 100 k points. A list of the extended Hückel parameters[16] follows:

atom	orbital	H_{ii}, eV	Slater exponents
C	2s	−21.4	1.625
	2p	−11.4	1.625
N	2s	−26.0	1.95
	2p	−13.4	1.95
H	1s	−13.6	1.3

Registry No. I (R = H), 128327-97-9; I (R = CH_3), 41209-65-8; I (R = *t*-Bu), 41205-71-4.

(25) Kroner, J.; Strack, W. *Angew. Chem., Int. Ed. Engl.* **1972**, *11*, 220.
(26) Ohsaku, M.; Sasaki, T.; Murata, H.; Imamura, A. *Eur. Polym. J.* **1981**, *17*, 913.